

IMPACT OF DIAPHRAGMS ON SEISMIC PERFORMANCE  
OF EXISTING SLAB-ON-GIRDER STEEL BRIDGES

by Seyed Mehdi Zahrai<sup>1</sup> and Michel Bruneau<sup>2</sup>

ABSTRACT

Many steel bridges have suffered damage during recent earthquakes (e.g. Northridge and Kobe). Reported instances of diaphragm damage include buckling of end-diaphragm braces, connection fractures of these braces and other non-ductile forms of damage. The absence of seismic ductile detailing provisions for steel bridges in all bridge design codes to date partly explains the observed behavior. Research was conducted to quantitatively investigate the impact of diaphragms on seismic response of slab-on-girder steel bridges and assess the actual vulnerability of these bridges to earthquakes due to various diaphragm conditions. Static and dynamic linear elastic as well as nonlinear inelastic seismic analyses were conducted. Typical 20 m to 60 m span slab-on-girder bridges have been considered, with and without web stiffeners and bracing systems. Simple hand-calculation analytical models were also developed to evaluate the lateral displacement and period of short to medium span slab-on-girder bridges with effective or ineffective end-diaphragms. Predictions from the simple models were in good agreement with those from computer analyses. Results from this analytical study also demonstrate that a small end-diaphragm stiffness is sufficient to make the entire superstructure behave as a unit in the elastic range. However, it is also shown that a considerable shift in seismic behavior occurs once rupture of end-diaphragms occurs, with a sizeable period elongation, considerably larger lateral displacements and higher propensity to damage due to P-A effects. It is also found that the presence of intermediate diaphragms does not significantly influence the seismic performance of these bridges, both in the elastic and inelastic range.

---

<sup>1</sup> Doctoral Candidate, Ottawa Carleton Earthquake Engineering Research Centre, Department of Civil Engineering, 161 Louis Pasteur, University of Ottawa, Ottawa, Ontario, Canada K1N 6N5. Tel.: (613) 562-5800 x 6159, Fax.: (613) 562-5173. Email: s058016@aix1.uottawa.ca

<sup>2</sup> Associate Professor, Ottawa Carleton Earthquake Engineering Research Centre, Department of Civil Engineering, 161 Louis Pasteur, University of Ottawa, Ottawa, Ontario, Canada K1N 6N5. Tel.: (613) 562-5800 x 6127, Fax.: (613) 562-5173. Email: bruneau@genie.uottawa.ca

### **Introduction: Current Research**

Several steel bridges have collapsed or suffered significant damage during recent earthquakes such as the 1989 Loma Prieta (Earthquake 1990), 1994 Northridge (Astaneh-Asl et al. 1994) and 1995 Kobe earthquakes (Bruneau et al. 1996). Although the potential seismic vulnerability of bridges, designed and constructed at a time when seismic-resistant provisions were nonexistent or ineffective, has long been recognized, these more recent failures have triggered considerable seismic evaluation and retrofit activities throughout North America, and generated renewed research interest on that subject. However, most of the current knowledge in earthquake-resistant bridge design is based on past studies of concrete bridges, and may require adjustments to effectively capture the seismic behavior germane to steel bridges. One such aspect of behavior is reviewed here.

Currently, in all available literature on the seismic evaluation and/or design of bridges (e.g. Seismic 1981; Ontario 1991; American 1994), when the lateral period of a slab-on-girder bridge is determined the superstructure is modelled as an equivalent beam supported on columns and/or foundation springs. The effective transverse stiffness of this equivalent beam is calculated considering that deck and girders act as a single cross-section. While this approach is acceptable for concrete bridges and box-girder superstructures, it may not be for some types of existing slab-on-girder steel bridges. Typically, in such bridges, the concrete deck is supported on I-shape beams interconnected by a few discrete diaphragms, and the mechanism by which the seismically-induced inertia forces at the concrete slab level will be transmitted to the girder bearings can be quite different from that assumed by the equivalent beam analogy. This difference depends on the diaphragm effectiveness, and can be quite large in bridges having flexible diaphragms. It is the objective of this paper to quantitatively investigate the lateral response of slab-on-girder steel bridges subjected to seismic lateral loads for various diaphragm conditions.

Here, a particular emphasis is placed on obtaining a proper representation of the superstructure's lateral stiffness as this has a direct impact on bridge period, and consequently on the intensity of earthquake excitation felt by the superstructure, bearings and substructure. To achieve this, the behavior of bridges with and without any effective diaphragms is first studied. Comprehensive analytical expressions that capture the behavior germane to slab-on-girder steel bridges as a function of end-diaphragm characteristics are presented. Finally elastic and inelastic analyses are conducted to validate the proposed models.

### **Description of the Selected Bridges**

Simply supported single-span bridges designed by Dicleli and Bruneau (1995) are considered for this study. To reflect the expected seismic performance of existing highway steel bridges, these bridges were designed to be in compliance with the strength requirements of the 1961 edition of the American Association of State Highway Officials (AASHTO) code (American, 1961). The characteristics of those bridges used in the current case study are listed in Table 1.

In all cases, 8 m wide two-lane bridges, supported by four 300W grade steel girders spaced at 2 m center-to-center are considered. The bridge deck consists of a 200 mm thick 20 MPa concrete slab

topped by 70 mm of asphalt. Finally, all bridges considered in this study do not have underside bracings; this was observed to be the case for those Eastern America bridges having rather weak diaphragms.

### **Slab-on-Girder Steel Bridges without Diaphragm**

For bridges without diaphragm, preliminary analyses revealed that the concrete deck responded as a nearly rigid member in the transverse direction, irrespectively of the pattern of the distributed lateral load applied. Hence, an equivalent static UDL (uniformly distributed load) applied at deck level was deemed representative of the seismically induced inertia forces acting on this bridge structure. In the following, a generic load level corresponding to a pseudo-acceleration of  $1g$  is considered.

The lateral response behavior of typical slab-on-girder steel bridges of various span lengths was first investigated using the program SAP90 (Wilson and Habibullah 1992). The resulting calculated first lateral period of vibration and resulting maximum drifts are presented as a function of span length in Figures 1a and 1 b, respectively.

It is noteworthy that the resulting lateral periods and maximum lateral deflections are very large compared to values typically reported for slab-on-girder bridges in the literature, reflecting the extreme flexibility of the structural system in absence of diaphragms. A typical deflected shape is presented in Figure 2, where side views at support and along span show a big difference in relative displacements. Clearly, the concrete deck slab displaces laterally nearly as a rigid body, while the flexible steel girders twist and deform laterally as necessary spanning between the slab and the supports. Closer examination of the steel beams reveals that they are most severely distorted near the supports; indeed, in each girder, the bearing supports are the only points which can counteract the lateral pull of the web to bring the lower flange under the slab. This visual observation of behavior has led to formulation of the proposed model described in the following section.

### **Proposed Model to Determine Period and Elastic Response**

Clearly, based on the above description of behavior, an appropriate model should consider the displacement of the deck slab relative to the bottom flange of girders, the web of girders providing a stiffness link between these two components. As a result, stresses in the webs vary greatly along the span. In fact, in each girder, web stresses will be largest at both ends where the bottom flange is restrained by the bearings, and will be minimum at midspan. Figures 2c and 2d show schematic simplified model of this behavior for slab-on-girder steel bridges without diaphragms.

Analytical expressions to calculate the lateral period and deformations of a bridge can be developed using this model. For that purpose, since the relative displacement between the deck slab and girders lower flanges plays a key role on behavior, it is convenient to define a relative displacement term,  $\Delta_r(x)$ , as:

$$\Delta_r(x) = \Delta_s - \Delta_b(x) \tag{1}$$

where  $\Delta_s$  and  $\Delta_b(x)$  are the slab and girders bottom flange displacements, respectively. The behavior of a bridge without diaphragm was found to resemble closely that of a beam on elastic foundation. In this analogy, the girder bottom flange and web respectively play the roles of the beam on a flexible surface and the springs of uniform stiffness. Therefore, the differential equation describing the bottom flange relative lateral displacement  $\Delta_r(x)$  is:

$$EI_b \frac{d^4 \Delta_r(x)}{dx^4} = -k_w \Delta_r(x) \quad (2)$$

where  $E$  is modulus of elasticity,  $I_b$  is the bottom flange moment of inertia about its strong axis and  $k_w$  is the web stiffness per unit length. If the bridge deck and bottom flanges can be assumed to remain always horizontal, the web stiffness can be modelled as:

$$k_w = \frac{12EI_w}{h_w^3} \quad (3)$$

where  $I_w$  is the web moment of inertia per unit length about the longitudinal axis of the bridge, and  $h_w$  is the web height between top and bottom flanges. In reality, SAP90 analyses of the bridges under lateral seismic loading reveal that while the deck remains relatively horizontal, the bottom flanges rotate and the above assumption makes the bridge slightly too stiff, but this is of little consequences in most cases as will be demonstrated later. If both ends of each bottom flange are simply supported in transverse direction, then  $\Delta_r(x)$  is:

$$\Delta_r(x) = \frac{2R_s \beta}{k_w} \frac{\cosh \beta x \cos \beta(L-x) + \cosh \beta(L-x) \cos \beta x}{\sin \beta L + \sinh \beta L} \quad (4)$$

where  $R_s$  is the support reaction resulting from bridge lateral loading tributary to one girder (based on the UDL applied at the deck level),  $L$  is the bridge span, and  $\beta$  is:

$$\beta = \sqrt[4]{\frac{k_w}{4EI_b}} \quad (5)$$

To obtain the fundamental lateral structural period, the generalized mass and stiffness,  $m^*$  and  $K^*$ , can be computed from the following:

$$m^* = \int_0^L \frac{m}{L} \Delta_s^2 dx = m \Delta_s^2 \quad (6)$$

$$K^* = n_g \left( \int_0^L \frac{12EI_w}{h_w^3} \Delta_r^2(x) dx + \int_0^L EI_b \Delta_b^2(x) dx \right) \quad (7)$$

where  $n_g$  is the number of girders and  $m$  is the entire bridge mass per unit length. Knowing that  $\Delta_r = \Delta_s$  at the supports ( $x=0$ ),  $R_s$  can be obtained as a function of  $\Delta_s$  from Eq. 4. In all cases, the lateral period of the bridge is given by:

$$T = 2\pi \sqrt{\frac{m^*}{K^*}} \quad (8)$$

The resulting periods and maximum drifts calculated according to this procedure are plotted in Figures 1a and 1b and compare well with the more accurate SAP90 results. In percentages, the difference between the results obtained using the proposed model and SAP90 increases as span length increases (Zahrai and Bruneau 1997). Figure 3 compares the lateral displacements of the bottom flange obtained using SAP90 and the proposed procedure, for 20 m span bridge. Result differences are mainly a consequence of neglecting bottom flange torsional rotations in the proposed model.

### **Nonlinear Inelastic Behavior**

ADINA (ADINA 1995) was used to investigate the nonlinear behavior of these steel bridges and the impact of P-A effects on this ultimate behavior. Results from push-over analyses shown in Figure 4 indicate that, since lateral displacements are large in bridges without any diaphragms, P-A effects due to the displaced weight of the deck are significant, leading to inelastic overturning and structural instability.

Inelastic analyses also reveal that, in the absence of end-diaphragms, the presence of intermediate diaphragms does not greatly improve the seismic behavior of slab-on-girder bridges as the largest girder web distortions occur nearer to the girder supports. To illustrate this phenomenon, a 40 m span bridge with intermediate diaphragms at every 8 m was considered. As shown in Figure 5, the impact of intermediate diaphragms in resisting the lateral loads is small. Note that as shown in Figure 3, the girder bottom flange can deform laterally further than the bridge deck in some locations. Consequently, the shear force resultant in some intermediate diaphragms can oppose that acting in the end-diaphragms or other intermediate diaphragms (Figure 5b).

### **Effect of Web Stiffeners**

Typically, bearing web stiffeners are needed at the supports of steel bridge girders to prevent web crippling and web buckling under gravity loads. Most existing bridges also have numerous intermediate transverse web stiffeners equally spaced along the length of girders and added to enhance the shear resistance of these girders. In view of the structural seismic behavior described above, and recognizing the role played by the web of girders, some special considerations are necessary to account for the presence of these stiffeners.

First, without changes to the above theory, the effect of equally distributed intermediate transverse web stiffeners can be directly considered by converting each stiffened web into an equivalent unstiffened web having a thickness chosen to give an identical transverse flexural stiffness.

Second, when the bearing stiffeners at the supports are larger than the distributed intermediate web stiffeners (as they frequently are), they effectively contribute an additional stiffness at each support, essentially acting as end-diaphragms, albeit weak ones. As bearing stiffeners can effectively be treated

as end-diaphragms, it is worthwhile to extend the above analytical study to parametrically include the stiffness contribution of end-diaphragms.

### Slab-on-Girder Steel Bridges with Effective Diaphragms

For bridges with diaphragms, preliminary analyses revealed that the concrete deck does not respond in a rigid-body motion during seismic excitations, as is the case for bridges without diaphragm. Rather, treating the structure as a generalized single-degree-of-freedom (SDOF), it was found appropriate to express the transverse response displacement mode shape of the bridge by a sine curve and find the effective forces corresponding to a generic pseudo acceleration of  $lg$ , accordingly (Zahrai and Bruneau 1997).

#### Proposed Model to Determine Period and Elastic Response

In the presence of end-diaphragms, the model previously derived must be modified to properly capture the lateral response of this type of steel bridge. The following mathematical approach was followed to develop an analytical expression capturing the lateral behavior of these steel bridges under transverse seismic excitation. The differential equation of motion for the bridge deck with continuous mass, neglecting the effects of shear strain and rotary inertia, can be written as:

$$-\frac{\partial^2 u(x,t)}{\partial t^2} = \frac{EI_D}{\rho A} \frac{\partial^4 u(x,t)}{\partial x^4} \quad (9)$$

where  $u(x,t)$  is a displacement function of the bridge deck in terms of longitudinal distance from the support,  $x$ , and time,  $t$ ,  $I_D$  is the superstructure moment of inertia (slab and girders acting as a unit) about a vertical axis perpendicular to the deck,  $\rho$  is mass density and  $A$  is the cross-sectional area of the entire superstructure. Hence,  $\rho A$  corresponds to the superstructure mass per unit length. As explained elsewhere (Zahrai and Bruneau 1997), by introducing a dimensionless parameter  $\alpha$ :

$$\alpha^4 = \frac{\rho A \omega^2 L^4}{EI_D} \quad (10)$$

the following expression for a steel bridge having end-diaphragms and assumed simply supported at both ends in the transverse direction, can be formed to obtain a by trial and error:

$$(K_b^*)^2 + \frac{\alpha^3(1+C_k)(\sinh\alpha \cos\alpha - \sin\alpha \cosh\alpha)}{2C_k \sin\alpha \sinh\alpha} K_b^* + \frac{\alpha^6(1 - \cos\alpha \cosh\alpha)}{2C_k \sin\alpha \sinh\alpha} \quad (11)$$

where  $C_k$  is the ratio of right to left end-diaphragm stiffnesses ( $K_{b2}/K_{b1}$ , usually 1.0), and  $K_b^*$ , the dimensionless stiffness, is:

$$K_b^* = \frac{K_b L^3}{EI_D} \quad (12)$$

in which,  $K_b$ , the stiffness of stiffened girders and lateral bracing systems at one end, depends on the geometry of the bridge and properties of the bearing stiffeners and diaphragm braces:

$$K_b = \sum_1^{n_g} \frac{12EI_s}{h_w^3} + \sum_1^{n_g-1} \frac{2EA_b \cos^2 \theta}{l_b} \quad (13)$$

where  $I_s$  is the moment of inertia of the bearing web stiffener about the longitudinal axis of the bridge,  $n_g$  is the number of girders,  $A_b$ ,  $l_b$  and  $\theta$  are the cross-sectional area, length and slope angle of braces. It is noteworthy that, in absence of diaphragm braces,  $K_b$  would simply be the lateral stiffness of transverse bearing web stiffeners, i.e.  $\sum 12EI_s/h_w^3$ . For example, with 100x10 stiffener plates on both sides of each girder web, in a 20 m span bridge having four girders,  $I_s$  and  $K_b$  would be  $7.8 \times 10^6 \text{ mm}^4$  and 170 kN/mm respectively. While, using X-shape braces of 2L100x100x10 between every two girders at bridge ends,  $K_b$  would be 1930 kN/mm (ignoring stiffeners), showing that braces create the main lateral stiffness for the bridge. In this case,  $K_b^*$  becomes 55.3, giving  $\alpha$  of 2.71 (Eq. 11). Finally, with  $I_D$  and  $\rho A$  of  $1.322 \text{ m}^4$  and 6300 kg/m respectively, a lateral period of 0.053 s (Eq. 10) is obtained.

### Numerical Examples

Using SAP90, the lateral period was computed for bridges with different spans, considering various X-braces as diaphragms. Note that many of the bridges' lower modes of vibration correspond to displacement response in the vertical direction: the discussion here addresses the lateral period corresponding to lateral response.

Figure 6 shows the resulting lateral period versus braces cross-sectional area, for 20 m, 40 m and 60m span bridges. If a zero cross-sectional area is assumed for the braces, periods of 0.82 s and 1.77 s are obtained respectively for 20 m and 60 m long bridges, i.e. the same values obtained before. By using 2L45x45x5 and 2L100x100x10 X-braces, lateral periods of 0.089 s and 0.052 s are obtained for the 20 m span bridge, and 0.24 s and 0.22 s respectively, for the 60 m span bridge. It is observed that a very small end-diaphragm is sufficient to produce a large "shift" in the period of these bridges, but that further increases in diaphragm stiffness have a marginal impact on lateral structural period.

Table 2 presents the lateral periods for all braced bridges considered in this study, and compares them with the periods obtained by SAP90. The difference between the results is smaller for larger span bridges, because shear deformations of the concrete deck are ignored in the proposed analytical model. For the 60m span bridge, where the shear to flexural deformation ratio is the lowest, the proposed hand-calculation analytical model offers the results closest to those obtained by SAP90.

### Nonlinear Inelastic Behavior

Frequently, end-diaphragms have sufficient strength to remain elastic during earthquakes, and brittle damage instead occurs in the diaphragm connections or elsewhere in the structure. However, to investigate whether intermediate diaphragms can effectively contribute to lateral load resistance when end-diaphragms undergo inelastic response, inelastic push-over analyses were carried out using ADINA. Results are shown in Figure 7 for 40 m span bridge having X-braces diaphragms between the girders, namely 2L65x65x6 for end-diaphragms and 2L45x45x5 for intermediate diaphragms. As shown in Figure 7, intermediate diaphragms only take a small percentage of the total applied load,

even after buckling and yielding of the end-diaphragm braces, and would remain elastic until very large ductilities develop in the end-diaphragms and at least until deck drifts in excess of 5%. Contribution of intermediate diaphragms is even less significant for the shorter bridges. This is because intermediate diaphragms are located 8 m from each other, the first one being at a greater percentage of the total span from the end in shorter bridges, and thus less likely to contribute being more remote from the zone of greater girder transverse deformation.

### **Conclusion**

The results of this limited analytical study demonstrate that a small end-diaphragm stiffness is sufficient to make the entire superstructure behave as a unit in the elastic range. However, the above results also clearly illustrate that a dramatic shift in seismic behavior will occur once rupture of those end-diaphragms occurs, with a sizeable period elongation, considerably larger lateral displacements and higher propensity to damage due to instability and P-A effects. It is also found that the presence of intermediate diaphragms does not significantly influence the seismic performance of these bridges, both in the elastic and inelastic range whether end-diaphragms are present or not.

Moreover, these analyses confirmed that effective end-diaphragms constitute critical structural elements along the main seismic load path, and that they should be designed accordingly. Therefore, in new bridges, they should be designed to resist in an elastic manner the forces induced by the maximum credible earthquake. Alternatively, they could be designed and detailed as ductile members to preclude brittle member or connections failure. This is not warranted for intermediate diaphragms. Non-ductile end-diaphragm members and connection details in existing steel bridges should be therefore retrofitted.

### **Acknowledgement**

The NSERC of Canada is acknowledged for its financial support. Also, the scholarship of the first author from the MCHE of Iran is highly appreciated. The findings and recommendations in this paper, however, are those of the writers, and not necessarily those of the sponsors.

### **References**

- ADINA R & D, Inc. (1995), "Automatic Dynamic Incremental Nonlinear Analysis", ADINA *software and documentations*, Watertown, MA.
- American Association of State Highway Officials (1961). *Standard specifications for highway bridges*, Washington, D.C.
- American Assoc. of State Highway and Transp. Officials (1994). *Standard specification for highway bridges*. Washington, D.C.
- Astaneh-Asl, A., Bolt, B., McMullin, K. M., Donikian, R. R., Modjtahedi, D. and Cho, S. W. (1994). "Seismic performance of steel bridges during the 1994 Northridge earthquake.", *UCB report CE-STEEL 94/01*, Berkeley, CA.

Bruneau, M., Wilson, J.W. and Tremblay, R. (1996). "Performance of steel bridges during the 1995 Hyogo-ken Nanbu (Kobe, Japan) earthquake.", *Canadian J. Civ. Engrg.*, 23(3), 678-713.

Dicleli, M., Bruneau, M. (1995). "Seismic performance of multi-span simply-supported slab-on-girder steel highway bridges.", *Engrg. Struct.*, 17(1), 4-14.

Earthquake Engineering Research Institute. (1990). "Loma Prieta Earthquake reconnaissance report." *Spectra*, Supplement to vol. 6, Oakland, CA.

Ontario Highway Bridge Design Code (1991). *Ministry of Transp.*, Quality and Standards Division, Ontario, Canada.

Seismic Design Guidelines for Highway Bridges (1981). *Report ATC-6*, Applied Technology Council, Redwood City, CA.

Wilson, E.L. and Habibullah, A. (1992). "SAP90 computer software for structural & earthquake engineering", *Computers & Structures Inc.*, Berkeley, CA.

Zahrai, S.M. And Bruneau, M. (1997). "Impact of Diaphragms on seismic response of slab-on-girder steel bridges", *J. Struct. Engrg.*, ASCE, Submitted for possible publication.

Table 1. Geometric and structural characteristics of the steel bridge considered in case studies where  $I_w$ ,  $I_b$  and  $I_D$  are the moments of inertia of girder web per unit length about bridge longitudinal axis, girder bottom flange about its strong axis, and superstructure about a vertical axis, respectively.

Span (m)	Deck Width (m)	No. of Girders	Girder Spacing (m)	Slab Depth (mm)	Girder Size and Properties	Mass ( $10^3$ kg)	$I_w$ ( $10^{-6}$ m <sup>4</sup> )	$I_b$ ( $10^{-6}$ m <sup>4</sup> )	$I_D$ (m <sup>4</sup> )
(1)	(2)	(3)	(4)	(5)	(6)	(7)	(9)	(8)	(10)
20	8	4	2	200	WWF800x184	126	0.111	56.25	1.322
30	8	4	2	200	WWF1000x262	202	0.229	133.3	1.617
40	8	4	2	200	WWF1200x333	286	0.341	160	1.797
50	8	4	2	200	WWF1400x405	367	0.341	312.5	1.983
60	8	4	2	200	WWF1600x496	465	0.341	485.3	2.212

Table 2. Lateral periods of braced bridges obtained by proposed method and SAP90 (assuming one laterally fixed end) where  $\rho A$  is the superstructure mass per unit length.

Bridge Span (m)	$\rho A$ (kg/m)	$I_D$ (m <sup>4</sup> )	X-braces size	$T_{SAP90}$ (s)	$T_{proposed}$ (s)	Difference (%)
(1)	(2)	(3)	(4)	(5)	(6)	(7)
20	6300	1.322	2L100x100x10	0.0515	0.047	8%
30	6733	1.617	2L100x100x10	0.076	0.071	7%
40	7150	1.797	2L100x100x10	0.12	0.112	6.6%
50	7340	1.983	2L100x100x10	0.17	0.16	6%
60	7750	2.212	2L100x100x10	0.222	0.213	4%

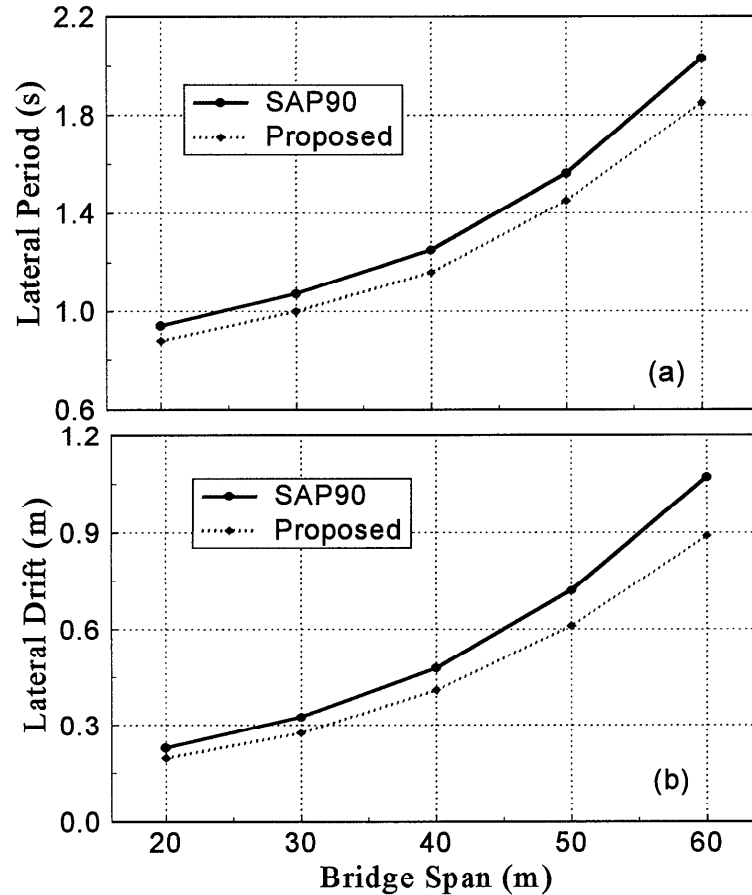


Figure 1. Comparison of results for different bridges (simply supported laterally) obtained by SAP90 and proposed model: a) Lateral Period, b) Lateral drift.

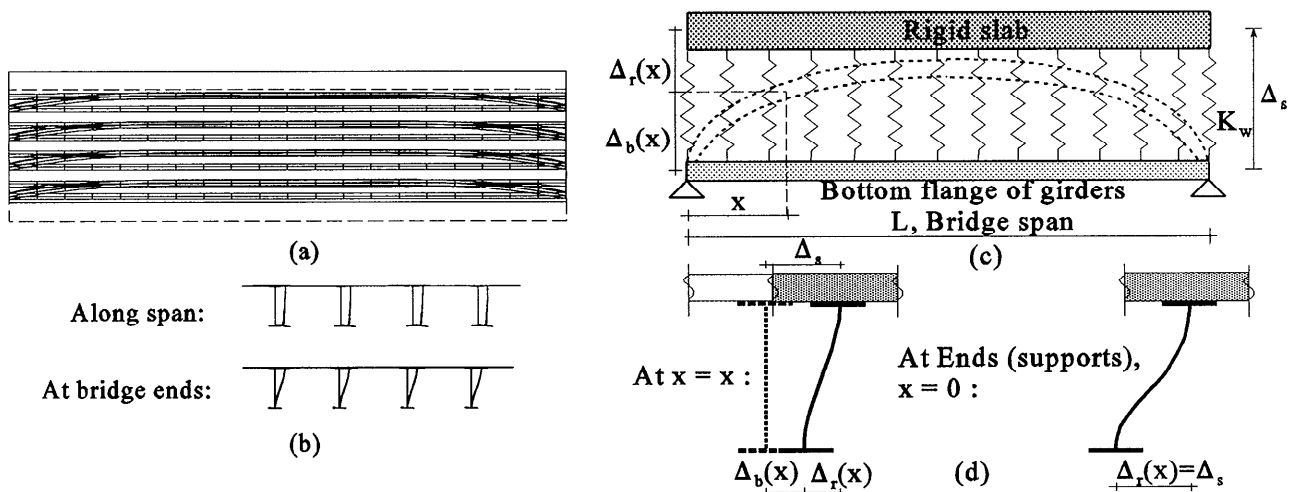


Figure 2. SAP90 deformed shapes of typical bridges without diaphragm: a) plain view, b) Side views; and schematic of simplified model without diagram: c) Plain view, d) Side views.

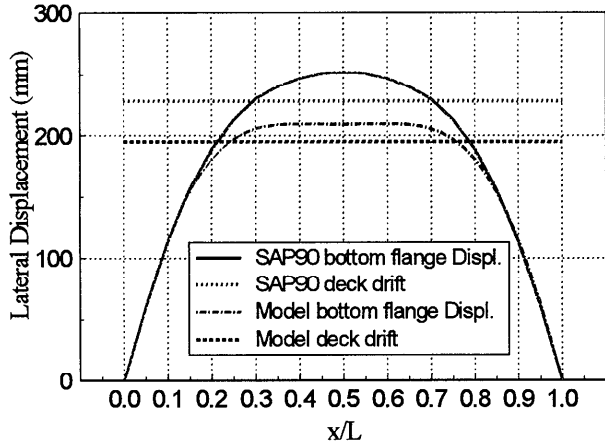


Figure 3. Comparison of girder bottom flange displacements by SAP90 and proposed model for the 20 m span bridge.

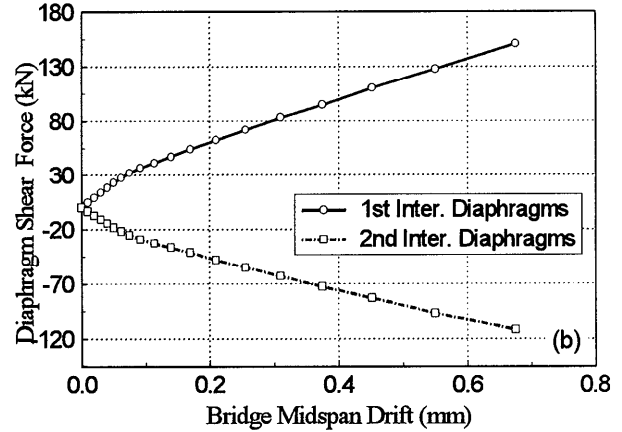
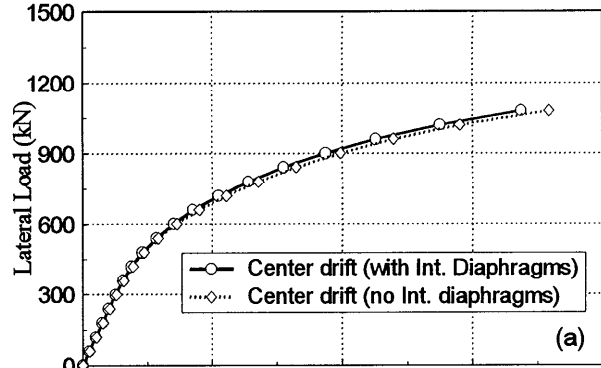


Figure 5. Impact of intermediate diaphragms on the 40 m span bridge without end-diaphragm: a) Lateral load versus midspan drift, and b) Horizontal shear force in braces of the first and second intermediate diaphragms from bridge end.

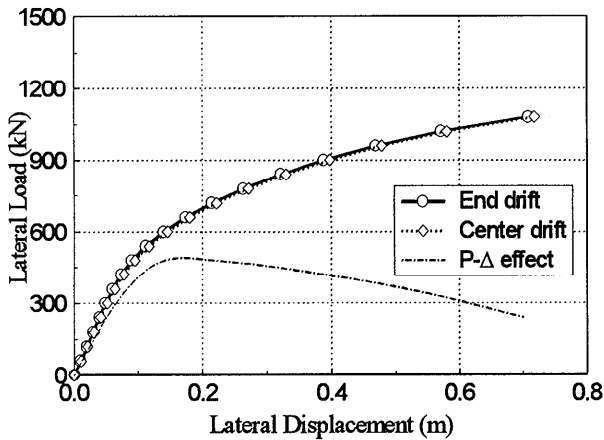


Figure 4. Load-displacement curve for the 40 m span bridge with and without consideration of P-A effect.

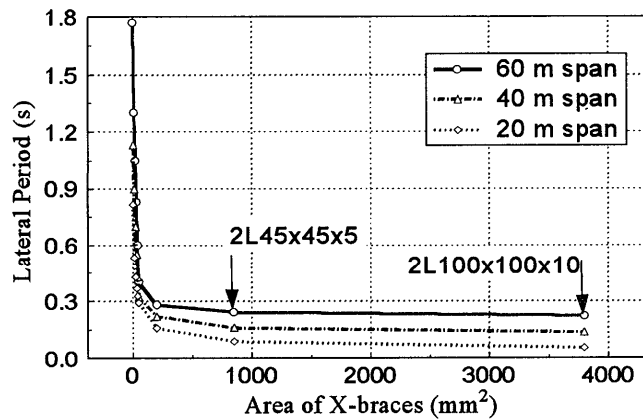


Figure 6. Lateral period versus cross-sectional area of braces for 20 m, 40 m and 60 m span bridges.

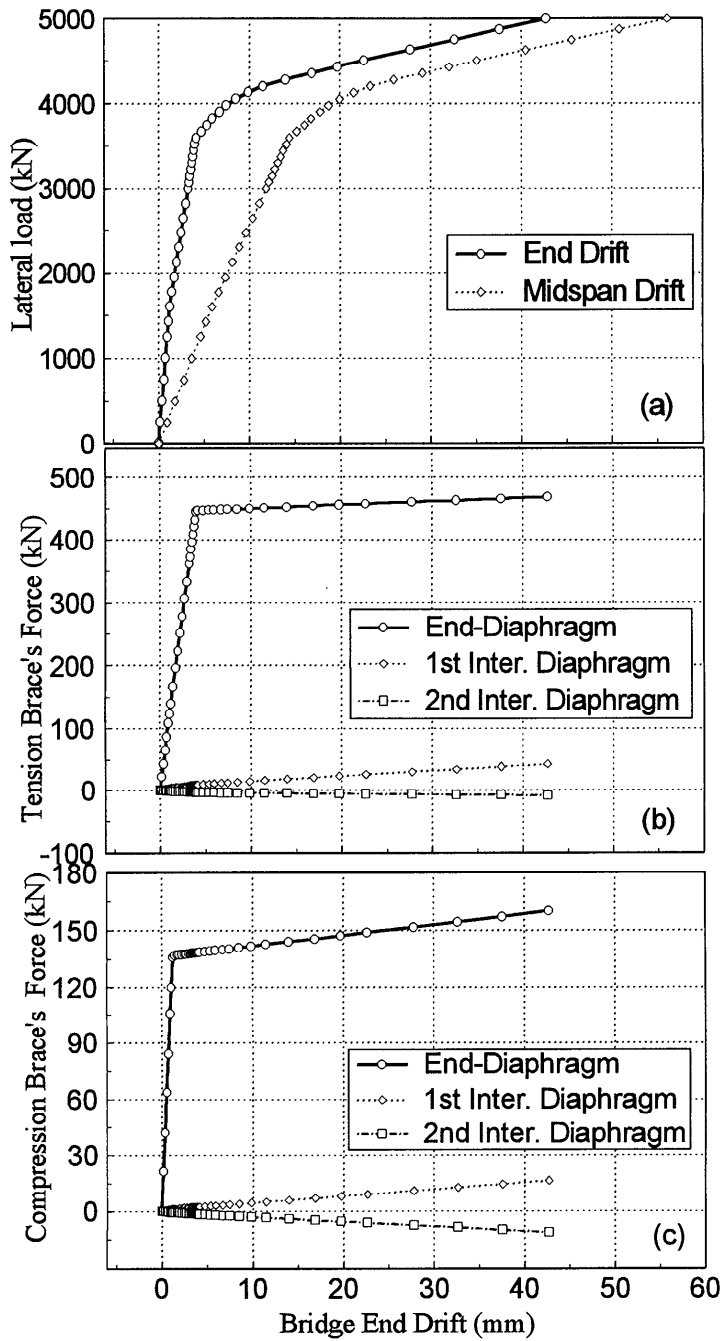


Figure 7. a) Lateral loads imposed to the braced 40 m span bridges versus end and midspan drifts; b) and c) Tension and compression axial forces in one pair of the diaphragm braces for the same bridge. Three pairs of braces are present in each diaphragm.